Chapter 5

Scaling FDTD Simulations to Any Frequency

5.1 Introduction

The FDTD method requires the discretization of time and space. Samples in time are Δ_t apart whereas, in simulations with one spatial dimension, samples in space are Δ_x apart. It thus appears that one must specify Δ_t and Δ_x in order to perform a simulation. However, as shown in Sec. 3.3, it is possible to write the coefficients $\Delta_t/\epsilon\Delta_x$ and $\Delta_t/\mu\Delta_x$ in terms of the material parameters and the Courant number (ref. (3.19) and (3.20)). Since the Courant number contains the ratio of the temporal step to the spatial step, it allows one to avoid explicitly stating a definite temporal or spatial step—all that matters is their ratio. This chapter continues to examine ways in which FDTD simulations can be treated as generic simulations that can be scaled to any size/frequency. As will be shown, the important factors which dictate the behavior of the fields in a simulation are the Courant number and the points per wavelength for any given frequency. We conclude the chapter by considering how one can obtain the transmission coefficient for a planar interface from a FDTD simulation.

5.2 Sources

5.2.1 Gaussian Pulse

In the previous chapters the source function, whether hardwired, additive, or incorporated in a TFSF formulation, was always a Gaussian. In the continuous world this function can be expressed as

$$f_g(t) = e^{-\left(\frac{t-d_g}{w_g}\right)^2} \tag{5.1}$$

where d_g is the temporal delay and w_g is a pulse-width parameter. The Gaussian has its peak value at $t = d_g$ (when the exponent is zero) and has a value of e^{-1} when $t = d_g \pm w_g$. Since (5.1) is only a function of time, i.e., a function of $q\Delta_t$ in the discretized world, it again appears as if the temporal step Δ_t must be given explicitly. However, if one specifies the delay and pulse width in

Lecture notes by John Schneider. `fdtd-dimensionless.tex`

terms of temporal steps, the term Δ_t appears in both the numerator and the denominator of the exponent. For example, in (3.29) d_g was $30\Delta_t$ and w_g was $10\Delta_t$ so the source function could be written

$$f_g(q\Delta_t) = f_g[q] = e^{-\left(\frac{q-30}{10}\right)^2}. \tag{5.2}$$

Note that Δ_t does not appear on the right-hand side.

As has been done previously, the discretized version of a function $f(q\Delta_t)$ will be written $f[q]$, i.e., the temporal step will be dropped from the argument since it does not appear explicitly in the expression for the function itself. The key to being able to discard Δ_t from the source function was the fact that the source parameters were all expressed in terms of the number of temporal steps.

5.2.2 Harmonic Sources

For a harmonic source, such as

$$f_h(t) = \cos(\omega t), \tag{5.3}$$

there is no explicit numerator and denominator in the argument. Replacing t with $q\Delta_t$ it again appears as if the temporal step must be given explicitly. However, keep in mind that with electromagnetic fields there is an explicit relationship between frequency and wavelength. For a plane wave propagating in free space, the wavelength λ and frequency f are related by

$$f\lambda = c \qquad \Rightarrow \qquad f = \frac{c}{\lambda}. \tag{5.4}$$

Thus the argument ωt (i.e., $2\pi f t$) can also be written as

$$\omega t = \frac{2\pi c}{\lambda} t. \tag{5.5}$$

For a given frequency, the wavelength is a fixed length. Being a length, it can be expressed in terms of the spatial step, i.e.,

$$\lambda = N_\lambda \Delta_x \tag{5.6}$$

where N_λ is the number of points per wavelength. This does not need to be an integer.

By relating frequency to wavelength and the wavelength to N_λ, the discretized version of the harmonic function can be written

$$f_h(q\Delta_t) = \cos\left(\frac{2\pi c}{N_\lambda \Delta_x} q\Delta_t\right) = \cos\left(\frac{2\pi}{N_\lambda}\frac{c\Delta_t}{\Delta_x} q\right), \tag{5.7}$$

or, simply,

$$f_h[q] = \cos\left(\frac{2\pi S_c}{N_\lambda} q\right). \tag{5.8}$$

The expression on the right now contains the Courant number and the parameter N_λ. In this form one does not need to state an explicit value for the temporal step. Rather, one specifies the Courant number S_c and the number of spatial steps per wavelength N_λ. Note that N_λ we will always be defined in terms of the number of spatial steps per the wavelength in free space. Furthermore, the wavelength is the one in the continuous world—we will see later that the wavelength in the FDTD grid is not always the same.

The period for a harmonic function is the inverse of the frequency

$$T = \frac{1}{f} = \frac{\lambda}{c} = \frac{N_\lambda \Delta_x}{c}. \tag{5.9}$$

The number of time steps in a period is thus given by

$$\frac{T}{\Delta_t} = \frac{N_\lambda \Delta_x}{c\Delta_t} = \frac{N_\lambda}{S_c}. \tag{5.10}$$

A harmonic wave traveling in the positive x direction is given by

$$f_h(x,t) = \cos(\omega t - kx) = \cos\left(\omega\left(t - \frac{k}{\omega}x\right)\right). \tag{5.11}$$

Since $k = \omega\sqrt{\mu_0\mu_r\epsilon_0\epsilon_r} = \omega\sqrt{\mu_r\epsilon_r}/c$, the argument can be written

$$\omega\left(t - \frac{k}{\omega}x\right) = \omega\left(t - \frac{\sqrt{\mu_r\epsilon_r}}{c}x\right). \tag{5.12}$$

Expressing all quantities in terms of the discrete values which pertain in the FDTD grid yields

$$\omega\left(t - \frac{\sqrt{\mu_r\epsilon_r}}{c}x\right) = \frac{2\pi c}{N_\lambda \Delta_x}\left(q\Delta_t - \frac{\sqrt{\mu_r\epsilon_r}}{c}m\Delta_x\right) = \frac{2\pi}{N_\lambda}(S_c q - \sqrt{\mu_r\epsilon_r}m). \tag{5.13}$$

Therefore the discretized form of (5.11) is given by

$$f_h[m,q] = \cos\left(\frac{2\pi}{N_\lambda}\left(S_c q - \sqrt{\mu_r\epsilon_r}m\right)\right). \tag{5.14}$$

This equation could now be used as the source in a total-field/scattered-field implementation. (However, note that when the temporal and spatial indices are zero this source has a value of unity. If that is the initial "turn-on" value of the source, that may cause artifacts which are undesirable. This will be considered further when dispersion is discussed. It is generally better to ramp the source up gradually. A simple improvement is offered by using a sine function instead of a cosine since sine is initially zero.)

5.2.3 The Ricker Wavelet

One of the features of the FDTD technique is that it allows the modeling of a broad range of frequencies using a single simulation. Therefore it is generally advantageous to use pulsed sources—which can introduce a wide spectrum of frequencies—rather than a harmonic source. The Gaussian pulse is potentially an acceptable source except that it contains a dc component. In fact, for a Gaussian pulse dc is the frequency with the greatest energy. Generally one would not use the FDTD technique to model dc fields. Sources with dc components also have the possibility of introducing artifacts which are not physical (e.g., charges which sit in the grid). Therefore we consider a different pulsed source which has no dc component and which can have its most energetic frequency set to whatever frequency (or discretization) is desired.

The Ricker wavelet is equivalent to the second derivative of a Gaussian; it is simple to implement; it has no dc component; and, its spectral content is fixed by a single parameter. The Ricker wavelet is often written

$$f_r(t) = \Big(1 - 2\big\{\pi f_P\,[t - d_r]\big\}^2\Big)\exp\Big(-\big\{\pi f_P\,[t - d_r]\big\}^2\Big) \tag{5.15}$$

where f_P is the "peak frequency" and d_r is the temporal delay. As will be more clear when the spectral representation of the function is shown below, the peak frequency is the frequency with the greatest spectral content.

The delay d_r can be set to any desired amount, but it is convenient to express it as a multiple of $1/f_P$, i.e.,

$$d_r = M_d \frac{1}{f_P} \tag{5.16}$$

where M_d is the delay multiple (which need not be an integer). An FDTD simulation is typically assumed to start at $t = 0$, but $f_r(t)$ is not zero for $t < 0$—rather $f_r(t)$ asymptotically approaches zero for large and small values of the argument, but never actually reaches zero (other than at two discrete zero-crossings). However, with a delay of $d_r = 1/f_P$ (i.e., $M_d = 1$), $|f_r(t < 0)|$ is bound by 0.001, which is small compared to the peak value of unity. Thus, the transient caused by "switching on" $f_r(t)$ at $t = 0$ is relatively small with this amount of delay. Said another way, since the magnitude of $f_r(t)$ is small for $t < 0$, these values can be approximated by assuming they are zero. For situations that may demand a smoother transition (i.e., a smaller initial turn-on value), the bound on $|f_r(t < 0)|$ can be made arbitrarily small by increasing d_r. For example, with a delay multiple M_d of 2, $|f_r(t < 0)|$ is bound by 10^{-15}.

The Fourier transform of (5.15) is

$$F_r(\omega) = -\frac{2}{f_P\sqrt{\pi}}\left(\frac{\omega}{2\pi f_P}\right)^2 \exp\left(-jd_r\omega - \left[\frac{\omega}{2\pi f_P}\right]^2\right). \tag{5.17}$$

Note that the delay d_r only appears as the imaginary part of the exponent. Thus it affects only the phase of $F_r(\omega)$, not the magnitude.

The functions $f_r(t)$ and $|F_r(\omega)|$ are shown in Fig. 5.1. For the sake of illustration, f_P is arbitrarily chosen to be 1 Hz and the delay is 1 s. Different values of f_P change the horizontal scale but they do not change the general shape of the curve. To obtain unit amplitude at the peak frequency, $F_r(\omega)$ has been scaled by $f_P e\sqrt{\pi}/2$.

The peak frequency f_P has a corresponding wavelength λ_P. This wavelength can be expressed in terms of the spatial step such that $\lambda_P = N_P\Delta_x$, where N_P does not need to be an integer. Thus

$$f_P = \frac{c}{\lambda_P} = \frac{c}{N_P\Delta_x} \tag{5.18}$$

The Courant number S_c is $c\Delta_t/\Delta_x$ so the spatial step can be expressed as $\Delta_x = c\Delta_t/S_c$. Using this in (5.18) yields

$$f_P = \frac{S_c}{N_P\Delta_t}. \tag{5.19}$$

The delay can thus be expressed as

$$d_r = M_d\frac{1}{f_P} = M_d\frac{N_P\Delta_t}{S_c}. \tag{5.20}$$

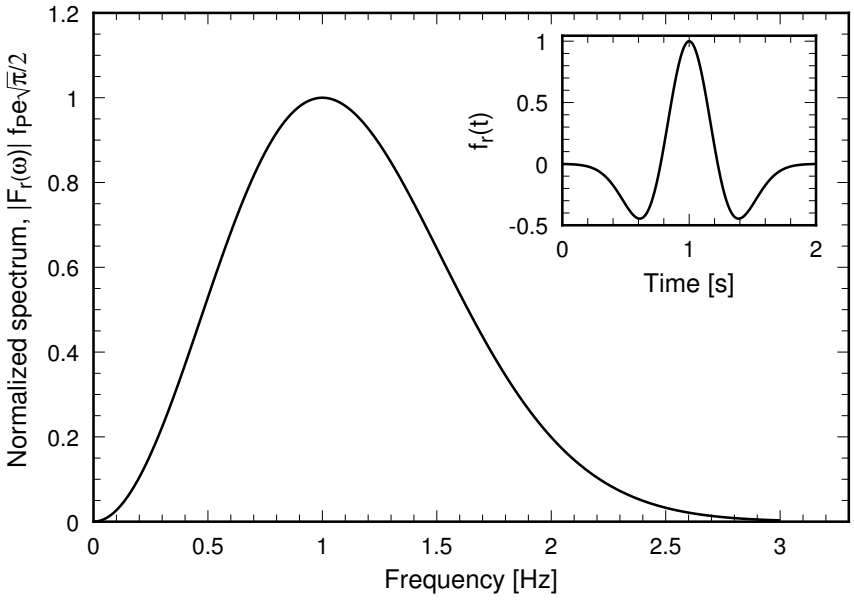

Figure 5.1: Normalized spectrum of the Ricker wavelet with $f_P = 1$ Hz. The corresponding temporal form $f_r(t)$ is shown in the inset box where a delay of 1 s has been assumed. For other values of f_P, the horizontal axis in the time domain is scaled by $1/f_P$. For example, if f_P were 1 MHz, the peak would occur at 1 μs rather than at 1 s. In the spectral domain, the horizontal axis is directly scaled by f_P so that if f_P were 1 MHz, the peak would occur at 1 MHz.

Letting time t be $q\Delta_t$ and expressing f_P and d_r as in (5.19) and (5.20), the discrete form of (5.15) can be written as

$$f_r[q] = \left(1 - 2\pi^2 \left[\frac{S_c q}{N_P} - M_d\right]^2\right) \exp\left(-\pi^2 \left[\frac{S_c q}{N_P} - M_d\right]^2\right). \tag{5.21}$$

Note that the parameters that specify $f_r[q]$ are the Courant number S_c, the points per wavelength at the peak frequency N_P, and the delay multiple M_d—there is no Δ_t in (5.21). This function appears to be independent of the temporal and spatial steps, but it does depend on their ratio via the Courant number S_c.

Equation (5.15) gives the Ricker wavelet as a function of only time. However, as was discussed in Sec. 3.10, when implementing a total-field/scattered-field boundary, it is necessary to parameterize an incident field in both time and space. As shown in Sec. 2.16, one can always obtain a traveling plane-wave solution to the wave equation simply by tweaking the argument of any function that is twice differentiable. Given the Ricker wavelet $f_r(t)$, $f_r(t \pm x/c)$ is a solution to the wave equation where c is the speed of propagation. The plus sign corresponds to a wave traveling in the negative x direction and the negative sign corresponds to a wave traveling in the positive x direction. (Although only 1D propagation will be considered here, this type of tweaking can also be done in 2D and 3D.) Therefore, a traveling Ricker wavelet can be constructed by replacing the argument t in (5.15) with $t \pm x/c$. The value of the function now depends on both time and

location, i.e., it is a function of two variables:

$$\begin{aligned} f_r(t \pm x/c) &= f_r(x,t), \\ &= \left(1 - 2\pi^2 f_P^2 \left[t \pm \frac{x}{c} - d_r\right]^2\right) \exp\left(-\pi^2 f_P^2 \left[t \pm \frac{x}{c} - d_r\right]^2\right). \end{aligned} \tag{5.22}$$

As before, (5.20) and (5.19) can be used to rewrite d_r and f_P in terms of the Courant number, the points per wavelength at the peak frequency, the temporal step, and the delay multiple. Replacing t with $q\Delta_t$, x with $m\Delta_x$, and employing the identity $x/c = m\Delta_x/c = m\Delta_t/S_c$, yields

$$f_r[m,q] = \left(1 - 2\pi^2 \left[\frac{S_c q \pm m}{N_P} - M_d\right]^2\right) \exp\left(-\pi^2 \left[\frac{S_c q \pm m}{N_P} - M_d\right]^2\right). \tag{5.23}$$

This gives the value of the Ricker wavelet at temporal index q and spatial index m. Note that when m is zero (5.23) reduces to (5.21).

5.3 Mapping Frequencies to Discrete Fourier Transforms

Assume the field was recorded during an FDTD simulation and then the recorded field was transformed to the frequency domain via a discrete Fourier transform. The discrete transform will yield a set of complex numbers that represents the amplitude of discrete spectral components. The question naturally arises: what is the correspondence between the indices of the transformed set and the actual frequency?

In any simulation, the highest frequency $f_{\max}$ that can exist is the inverse of the shortest period that can exist. In a discrete simulation one must have at least two samples per period. Since the time samples are Δ_t apart, the shortest possible period is $2\Delta_t$. Therefore

$$f_{\max} = \frac{1}{2\Delta_t}. \tag{5.24}$$

The change in frequency from one discrete frequency to the next is the spectral resolution Δ_f. The spectral resolution is dictated by the total number of samples which we will call N_T (an integer value). In general N_T would correspond to the number of time steps in an FDTD simulation. The spectral resolution is given by

$$\Delta_f = \frac{f_{\max}}{N_T/2}. \tag{5.25}$$

The factor of two is a consequence of the fact that there are both positive and negative frequencies. Thus one can think of the entire spectrum as ranging from $-f_{\max}$ to $f_{\max}$, i.e., an interval of $2f_{\max}$ which is then divided by N_T. Alternatively, to find Δ_f we can divide the maximum positive frequency by $N_T/2$ as done in (5.25). Plugging (5.24) into (5.25) yields

$$\Delta_f = \frac{1}{N_T \Delta_t}. \tag{5.26}$$

In Sec. 5.2.2 it was shown that a given frequency f could be written $c/\lambda = c/N_\lambda \Delta_x$ where N_λ is the number of points per wavelength (for the free-space wavelength). After transforming to the

spectral domain, this frequency would have a corresponding index given by

$$N_{\text{freq}} = \frac{f}{\Delta_f} = \frac{N_T c \Delta_t}{N_\lambda \Delta_x} = \frac{N_T}{N_\lambda} \frac{c\Delta_t}{\Delta_x} = \frac{N_T}{N_\lambda} S_c. \tag{5.27}$$

Thus, the spectral index is dictated by the duration of the simulation N_T, the Courant number S_c, and the points per wavelength N_λ.

Note that in practice different software packages may index things differently. The most typical practice is to have the first element in the spectral array correspond to dc, the next $N_T/2$ elements correspond to the positive frequencies, and then the next $(N_T/2) - 1$ elements correspond to the negative frequencies (which will always be the complex conjugates of the positive frequencies in any real FDTD simulation). The negative frequencies typically are stored from highest frequency to lowest (i.e., fastest varying to slowest) so that the last value in the array corresponds to the negative frequency closest to dc ($-\Delta_f$). Additionally, note that in (5.27) dc corresponds to an N_{freq} of zero (since N_λ is infinity for dc). However when using Matlab the dc term in the array obtained using the `fft()` command has an index of one. The first element in the array has an index of one—there is no "zero" element in Matlab arrays. So, one must understand and keep in mind the implementation details for a given software package.

From (5.19), the most energetic frequency in a Ricker wavelet can be written

$$f_P = \frac{S_c}{N_P \Delta_t}. \tag{5.28}$$

The spectral index corresponding to this is given by

$$N_{\text{freq}} = \frac{f_P}{\Delta_f} = \frac{N_T}{N_P} S_c. \tag{5.29}$$

This is identical to (5.27) except the generic value N_λ has been replaced by N_P which is the points per wavelength at the peak frequency.

A discrete Fourier transform yields an array of numbers which inherently has integer indices. The array elements correspond to discrete frequencies at multiples of Δ_f. However, N_{freq} given in (5.27) need not be thought of as an integer value. As an example, assume there were 65536 times steps in a simulation in which the Courant number was $1/\sqrt{2}$. Further assume that we are interested in the frequency which corresponds to 30 points per wavelength ($N_\lambda = 30$). In this case N_{freq} equals $65536/(30\sqrt{2}) = 1544.6983\cdots$. There is no reason why one cannot think in terms of this particular frequency. However, this frequency is not directly available from a discrete Fourier transform of the temporal data since the transform will only have integer values of N_{freq}. For this simulation an N_{freq} of 1544 corresponds $30.0136\cdots$ points per wavelength while an N_{freq} of 1545 corresponds $29.9941\cdots$ points per wavelength. One can interpolate between these values if the need is to measure the spectral output right at 30 points per wavelength.

5.4 Running Discrete Fourier Transform (DFT)

If one calculates the complete Fourier transform of the temporal data of length N_T points, one obtains information about the signal at N_T distinct frequencies (if one counts both positive and

negative frequencies). However, much of that spectral information is of little practical use. Because of the dispersion error inherent in the FDTD method and other numerical artifacts, one does not trust results which correspond to frequencies with too coarse a discretization. When taking the complete Fourier transform one often relies upon a separate software package such as Mathematica, Matlab, or perhaps the FFTw routines (a suite of very good C routines to perform discrete Fourier transforms). However, if one is only interested in obtaining spectral information at a few frequencies, it is quite simple to implement a discrete Fourier transform (DFT) which can be incorporated directly into the FDTD code. The DFT can be performed as the simulation progresses and hence the temporal data does not have to be recorded. This section outlines the steps involved in computing such a "running DFT."

Let us consider a discrete signal $g[q]$ which is, at least in theory, periodic with a period of N_T so that $g[q] = g[q+N_T]$ (in practice only one period of the signal is of interest and this corresponds to the data obtained from an FDTD simulation). The discrete Fourier series representation of this signal is

$$g[q] = \sum_{k=\langle N_T \rangle} a_k e^{jk(2\pi/N_T)q} \tag{5.30}$$

where k is an integer index and

$$a_k = \frac{1}{N_T} \sum_{q=\langle N_T \rangle} g[q] e^{-jk(2\pi/N_T)q} \tag{5.31}$$

The summations are taken over N_T consecutive points—we do not care which ones, but in practice for our FDTD simulations a_k would be calculated with q ranging from 0 to $N_T - 1$ (the term below the summation symbols in (5.30) and (5.31) indicates the summations are done over N_T consecutive integers, but the actual start and stop points do not matter). The term a_k gives the spectral content at the frequency $f = k\Delta_f = k/(N_T\Delta_t)$. Note that a_k is obtained simply by taking the sum of the sequence $g[q]$ weighted by an exponential.

The exponential in (5.31) can be written in terms of real and imaginary parts, i.e.,

$$\Re[a_k] = \frac{1}{N_T} \sum_{q=0}^{N_T-1} g[q] \cos\left(\frac{2\pi k}{N_T} q\right), \tag{5.32}$$

$$\Im[a_k] = -\frac{1}{N_T - 1} \sum_{q=0}^{N_T} g[q] \sin\left(\frac{2\pi k}{N_T} q\right), \tag{5.33}$$

where $\Re[]$ indicates the real part and $\Im[]$ indicates the imaginary part. In practice, $g[q]$ would be a particular field component and these calculations would be performed concurrently with the time-stepping. The value of $\Re[a_k]$ would be initialized to zero. Then, at each time step $\Re[a_k]$ would be set equal to its previous value plus the current value of $g[q]\cos(2\pi kq/N_T)$, i.e., we would perform a running sum. Once the time-stepping has completed, the stored value of $\Re[a_k]$ would be divided by N_T. A similar procedure is followed for $\Im[a_k]$ where the only difference is that the value used in the running sum is $-g[q]\sin(2\pi kq/N_T)$. Note that the factor $2\pi k/N_T$ is a constant for a particular frequency, i.e., for a particular k.

Similar to the example at the end of the previous section, let us consider how we would extract information at a few specific discretizations. Assume that $N_T = 8192$ and $S_c = 1/\sqrt{2}$. Further

assume we want to find the spectral content of a particular field for discretizations of $N_\lambda = 20$, 30, 40, and 50 points per wavelength. Plugging these values into (5.27) yields corresponding spectral indices (i.e., N_{freq} or index k in (5.31)) of

$$\begin{aligned} N_\lambda = 20 &\Rightarrow k = 289.631, \\ N_\lambda = 30 &\Rightarrow k = 193.087, \\ N_\lambda = 40 &\Rightarrow k = 144.815, \\ N_\lambda = 50 &\Rightarrow k = 115.852. \end{aligned}$$

The spectral index must be an integer. Therefore, rounding k to the nearest integer and solving for the corresponding N_λ we find

$$\begin{aligned} k = 290 &\Rightarrow N_\lambda = 19.9745, \\ k = 193 &\Rightarrow N_\lambda = 30.0136, \\ k = 145 &\Rightarrow N_\lambda = 39.9491, \\ k = 116 &\Rightarrow N_\lambda = 49.9364. \end{aligned}$$

Note that these values of N_λ differ slightly from the "desired" values. Assume that we are modeling an object with some characteristic dimension of twenty cells, i.e., $a = 20\Delta_x$. Given the initial list of integer N_λ values, we could say that we were interested in finding the field at frequencies with corresponding wavelengths of a, $\frac{3}{2}a$, $2a$, and $\frac{5}{2}a$. However, using the non-integer N_λ's that are listed above, the values we obtain correspond to $0.99877a$, $1.500678a$, $1.997455a$, and $2.496818a$. As long as one is aware of what is actually being calculated, this should not be a problem. Of course, as mentioned previously, if we want to get closer to the desired values, we can interpolate between the two spectral indices which bracket the desired value.

5.5 Real Signals and DFT's

In nearly all FDTD simulations we are concerned with real signals, i.e., $g[q]$ in (5.30) and (5.31) are real. For a given spectral index k (which can be thought of as a frequency), the spectral coefficient a_k is as given in (5.31). Now, consider an index of $N_T - k$. In this case the value of a_{N_T-k} is given by

$$\begin{aligned} a_{N_T-k} = &= \frac{1}{N_T} \sum_{q=\langle N_T \rangle} g[q] e^{-j(N_T-k)(2\pi/N_T)q}, \\ &= \frac{1}{N_T} \sum_{q=\langle N_T \rangle} g[q] e^{-j2\pi} e^{jk(2\pi/N_T)q}, \\ &= \frac{1}{N_T} \sum_{q=\langle N_T \rangle} g[q] e^{jk(2\pi/N_T)q}, \\ a_{N_T-k} &= a_k^*, \end{aligned} \tag{5.34}$$

where a_k^* is the complex conjugate of a_k. Thus, for real signals, the calculation of one value of a_k actually provides the value of two coefficients: the one for index k and the one for index $N_T - k$.

Another important thing to note is that, similar to the continuous Fourier transform where there are positive and negative frequencies, with the discrete Fourier transform there are also pairs of frequencies that should typically be considered together. Let us assume that index k goes from 0 to $N_T - 1$. The $k = 0$ frequency is dc. Assuming N_T is even, $k = N_T/2$ is the Nyquist frequency where the spectral basis function $\exp(j\pi q)$ alternates between positive and negative one at each successive time-step. Both a_0 and $a_{N_T/2}$ will be real. All other spectral components can be complex, but for real signals it will always be true that $a_{N_T-k} = a_k^*$.

If we are interested in the amplitude of a spectral component at a frequency of k, we really need to consider the contribution from both k and $N_T - k$ since the oscillation at both these indices is at the same frequency. Let us assume we are interested in reconstructing just the k'th frequency of a signal. The spectral components would be given in the time domain by

$$\begin{aligned} f[q] &= a_{k'} e^{jk'(2\pi/N_T)q} + a_{N_T-k'} e^{j(N_T-k')(2\pi/N_T)q} \\ &= a_{k'} e^{jk'(2\pi/N_T)q} + a_{k'}^* e^{j2\pi} e^{-jk'(2\pi/N_T)q} \\ &= 2\Re[a_{k'}] \cos\left(\frac{2k'\pi}{N_T} q\right) - 2\Im[a_{k'}] \sin\left(\frac{2k'\pi}{N_T} q\right) \\ &= 2|a_{k'}| \cos\left(\frac{2k'\pi}{N_T} q + \tan^{-1}\left(\frac{\Im[a_{k'}]}{\Re[a_{k'}]}\right)\right) \end{aligned} \tag{5.35}$$

Thus, importantly, the amplitude of this harmonic function is given by $2|a_{k'}|$ (and not merely $|a_{k'}|$).

Let us explore this further by considering the x component of an electric field at some arbitrary point that is given by

$$\begin{aligned} \mathbf{E}[q] &= E_{x0} \cos[\omega_{k'} q + \theta_e] \hat{\mathbf{a}}_x, \\ &= \Re[E_{x0} e^{j\theta_e} e^{j\omega_{k'} q}] \hat{\mathbf{a}}_x, \\ &= \frac{1}{2}[\hat{E}_{x0} e^{j\omega_{k'} q} + \hat{E}_{x0}^* e^{-j\omega_{k'} q}] \hat{\mathbf{a}}_x, \end{aligned} \tag{5.36}$$

where

$$\omega_{k'} = k' \frac{2\pi}{N_T}, \tag{5.37}$$

$$\hat{E}_{x0} = E_{x0} e^{j\theta_e}, \tag{5.38}$$

and k' is some arbitrary integer constant. Plugging (5.36) into (5.31) and dropping the unit vector yields

$$\begin{aligned} a_k &= \frac{1}{2N_T} \sum_{q=\langle N_T \rangle} [\hat{E}_{x0} e^{j\omega_{k'} q} + \hat{E}_{x0}^* e^{-j\omega_{k'} q}] e^{-j\omega_k q}, \\ &= \frac{1}{2N_T} \sum_{q=\langle N_T \rangle} [\hat{E}_{x0} e^{j(\omega_{k'} - \omega_k) q} + \hat{E}_{x0}^* e^{-j(\omega_{k'} + \omega_k) q}], \\ &= \frac{1}{2N_T} \sum_{q=\langle N_T \rangle} [\hat{E}_{x0} e^{j(k'-k)(2\pi/N_T) q} + \hat{E}_{x0}^* e^{-j(k'+k)(2\pi/N_T) q}]. \end{aligned} \tag{5.39}$$

Without loss of generality, let us now assume q varies between 0 and $N_T - 1$ while k and k' are restricted to be between 0 and $N_T - 1$. Noting the following relationship for geometric series

$$\sum_{q=0}^{N-1} x^q = 1 + x + x^2 + \cdots + x^{N-1} = \frac{1 - x^N}{1 - x} \tag{5.40}$$

we can express the sum of the first exponential expression in (5.39) as

$$\sum_{q=0}^{N_T-1} e^{j(k'-k)(2\pi/N_T)q} = \frac{1 - e^{j(k'-k)2\pi}}{1 - e^{j(k'-k)(2\pi/N_T)}}. \tag{5.41}$$

Since k and k' are integers, the second term in the numerator on the right side, $\exp(j(k' - k)2\pi)$, equals 1 for all values of k and k' and thus this numerator is always zero. Provided $k \neq k'$, the denominator is non-zero and we conclude that for $k \neq k'$ the sum is zero. For $k = k'$, the denominator is also zero and hence the expression on the right does not provide a convenient way to determine the value of the sum. However, when $k = k'$ the terms being summed are simply 1 for all values of q. Since there are N_T terms, the sum is N_T. Given this, we can write the "orthogonality relationship" for the exponentials

$$\sum_{q=0}^{N_T-1} e^{j(k'-k)(2\pi/N_T)q} = \begin{cases} 0 & k' \neq k \\ N_T & k' = k \end{cases} \tag{5.42}$$

Using this orthogonality relationship in (5.39), we find that for the harmonic signal given in (5.36), one of the non-zero spectral coefficients is

$$a_{k'} = \frac{1}{2}\hat{E}_{x0}. \tag{5.43}$$

Conversely, expressing the (complex) amplitude in terms of the spectral coefficient from the DFT, we have

$$\hat{E}_{x0} = 2a_{k'}. \tag{5.44}$$

For the sake of completeness, now consider the sum of the other complex exponential term in (5.39). Here the orthogonality relationship is

$$\sum_{q=0}^{N_T-1} e^{-j(k'+k)(2\pi/N_T)q} = \begin{cases} 0 & k \neq N_T - k' \\ N_T & k = N_T - k' \end{cases} \tag{5.45}$$

Using this in (5.39) tells us

$$a_{N_T-k'} = \frac{1}{2}\hat{E}^*_{x0}. \tag{5.46}$$

Or, expressing the (complex) amplitude in terms of this spectral coefficient from the DFT, we have

$$\hat{E}_{x0} = 2a^*_{N_T-k'}. \tag{5.47}$$

Now, let us consider the calculation of the time-averaged Poynting vector $\mathbf{P}_{avg}$ which is given by

$$\mathbf{P}_{\text{avg}} = \frac{1}{2}\Re\left[\hat{\mathbf{E}} \times \hat{\mathbf{H}}^*\right] \tag{5.48}$$

where the carat indicates the phasor representation of the field, i.e.,

$$\begin{aligned}\hat{\mathbf{E}} &= \hat{E}_{x0}\hat{\mathbf{a}}_x + \hat{E}_{y0}\hat{\mathbf{a}}_y + \hat{E}_{z0}\hat{\mathbf{a}}_z, \\ &= 2a_{e,x,k}\hat{\mathbf{a}}_x + 2a_{e,y,k}\hat{\mathbf{a}}_y + 2a_{e,z,k}\hat{\mathbf{a}}_z \end{aligned} \tag{5.49}$$

where $a_{e,w,k}$ is the kth spectral coefficient for the w component of the electric field with $w \in \{x, y, z\}$. Defining things similarly for the magnetic field yields

$$\begin{aligned}\hat{\mathbf{H}} &= \hat{H}_{x0}\hat{\mathbf{a}}_x + \hat{H}_{y0}\hat{\mathbf{a}}_y + \hat{H}_{z0}\hat{\mathbf{a}}_z, \\ &= 2a_{h,x,k}\hat{\mathbf{a}}_x + 2a_{h,y,k}\hat{\mathbf{a}}_y + 2a_{h,z,k}\hat{\mathbf{a}}_z. \end{aligned} \tag{5.50}$$

The time-averaged Poynting vector can now be written in terms of the spectral coefficients as

$$\begin{aligned}\mathbf{P}_{avg} = 2\,\Re\Big[&\left[a_{e,y,k}a^*_{h,z,k} - a_{e,z,k}a^*_{h,y,k}\right]\hat{\mathbf{a}}_x + \left[a_{e,z,k}a^*_{h,x,k} - a_{e,x,k}a^*_{h,z,k}\right]\hat{\mathbf{a}}_y + \\ &\left[a_{e,x,k}a^*_{h,y,k} - a_{e,y,k}a^*_{h,x,k}\right]\hat{\mathbf{a}}_z\Big]. \end{aligned} \tag{5.51}$$

Thus, importantly, when directly using these DFT coefficients in the calculation of the Poynting vector, instead of the usual "one-half the real part of E cross H," the correct expression is "two times the real part of E cross H."

5.6 Amplitude and Phase from Two Time-Domain Samples

In some applications the FDTD method is used in a quasi-harmonic way, meaning the source is turned on, or ramped up, and then run continuously in a harmonic way until the simulation is terminated. Although this prevents one from obtaining broad spectrum output, for applications that have highly inhomogeneous media and where only a single frequency is of interest, the FDTD method used in a quasi-harmonic way may still be the best numerical tool to analyze the problem. The FDTD method is often used in this when in the study of the interaction of electromagnetic fields with the human body. (Tissues in the human body are typically quite dispersive. Implementing dispersive models that accurately describe this dispersion over a broad spectrum can be quite challenging. When using a quasi-harmonic approach one can simply use constant coefficients for the material constants, i.e., use the values that pertain at the frequency of interest which also corresponds to the frequency of the excitation.)

When doing a quasi-harmonic simulation, the simulation terminates when the fields have reached steady state. Steady state can be defined as the time beyond which temporal changes in the amplitude and phase of the fields are negligibly small. Thus, one needs to know the amplitude and phase of the fields at various points. Fortunately the amplitude and phase can be calculated from only two sample points of the time-domain field.

Let us assume the field at some point (x, y, z) is varying harmonically as

$$f(x, y, z, t) = A(x, y, z)\cos(\omega t + \phi(x, y, z)). \tag{5.52}$$

where A is the amplitude and ϕ is the phase, both of which are initially unknown. We will drop the explicit argument of space in the following with the understanding that we are talking about the field at a fixed point.

Consider two different samples of the field in time

$$f(t_1) = f_1 = A\cos(\omega t_1 + \phi), \tag{5.53}$$
$$f(t_2) = f_2 = A\cos(\omega t_2 + \phi). \tag{5.54}$$

We will assume that the samples are taken roughly a quarter of a cycle apart to ensure the samples are never simultaneously zero. A quarter of a cycle is given by $T/4$ where T is the period. We can express this in terms of time steps as

$$\frac{T}{4} = \frac{1}{4f} = \frac{\lambda}{4c} = \frac{N_\lambda \Delta_x}{4c}\frac{\Delta_t}{\Delta_t} = \frac{N_\lambda}{4S_c}\Delta_t. \tag{5.55}$$

Since we only allow an integer number of time-steps between t_1 and t_2, the temporal separation between t_1 and t_2 would be int$(N_\lambda/4S_c)$ time-steps.

Given these two samples, f_1 and f_2, we wish to determine A and ϕ. Using the trig identity for the cosine of the sum of two values, we can express these fields as

$$f_1 = A(\cos(\omega t_1)\cos(\phi) - \sin(\omega t_1)\sin(\phi)), \tag{5.56}$$
$$f_2 = A(\cos(\omega t_2)\cos(\phi) - \sin(\omega t_2)\sin(\phi)). \tag{5.57}$$

We are assuming that f_1 and f_2 are known and we know the times at which the samples were taken. Using (5.56) to solve for A we obtain

$$A = \frac{f_1}{\cos(\omega t_1)\cos(\phi) - \sin(\omega t_1)\sin(\phi)}. \tag{5.58}$$

Plugging (5.58) into (5.57) and rearranging terms ultimately leads to

$$\frac{\sin(\phi)}{\cos(\phi)} = \tan(\phi) = \frac{f_2\cos(\omega t_1) - f_1\cos(\omega t_2)}{f_2\sin(\omega t_1) - f_1\sin(\omega t_2)}. \tag{5.59}$$

The time at which we take the first sample, t_1, is almost always arbitrary. We are free to call that "time zero," i.e., $t_1 = 0$. By doing this we have $\cos(\omega t_1) = 1$ and $\sin(\omega t_1) = 0$. Using these values in (5.59) and (5.58) yields

$$\phi = \tan^{-1}\left(\frac{\cos(\omega t_2) - \frac{f_2}{f_1}}{\sin(\omega t_2)}\right), \tag{5.60}$$

and

$$A = \frac{f_1}{\cos(\phi)}. \tag{5.61}$$

Note that these equations assume that $f_1 \neq 0$ and, similarly, that $\phi \neq \pm\pi/2$ radians (which is the same as requiring that $\cos(\phi) \neq 0$).

If f_1 is identically zero, we can say that ϕ is $\pm\pi/2$ (where the sign can be determined by the other sample point: $\phi = -\pi/2$ if $f_2 > 0$ and $\phi = +\pi/2$ if $f_2 < 0$). If f_1 is not identically zero, we can use (5.60) to calculate the phase since the inverse tangent function has no problem with large arguments. However, if the phase is close to $\pm\pi/2$, the amplitude as calculated by (5.61) would

involve the division of two small numbers which is generally not a good way to determine a value. Rather than doing this, we can use (5.57) to express the amplitude as

$$A = \frac{f_2}{\cos(\omega t_2)\cos(\phi) - \sin(\omega t_2)\sin(\phi)}. \tag{5.62}$$

This equation should perform well when the phase is close to $\pm\pi/2$.

At this point we have the following expressions for the phase and magnitude (the reason for adding a prime to the phase and magnitude will become evident shortly):

$$\phi' = \begin{cases} -\pi/2 & \text{if } f_1 = 0 \text{ and } f_2 > 0 \\ \pi/2 & \text{if } f_1 = 0 \text{ and } f_2 < 0 \\ \tan^{-1}\left(\frac{\cos(\omega t_2) - \frac{f_2}{f_1}}{\sin(\omega t_2)}\right) & \text{otherwise} \end{cases} \tag{5.63}$$

and

$$A' = \begin{cases} \frac{f_1}{\cos(\phi')} & \text{if } |f_1| \geq |f_2| \\ \frac{f_2}{\cos(\omega t_2)\cos(\phi') - \sin(\omega t_2)\sin(\phi')} & \text{otherwise} \end{cases} \tag{5.64}$$

There is one final step in calculating the magnitude and phase. The inverse-tangent function returns values between $-\pi/2$ and $\pi/2$. As given by (5.64), the amplitude A' can be either positive or negative. Generally we think of phase as varying between $-\pi$ and π and assume the amplitude is non-negative. To obtained such values we can obtain the final values for the amplitude and phase as follows

$$(A, \phi) = \begin{cases} (A', \phi') & \text{if } A' > 0 \\ (-A', \phi' - \pi) & \text{if } A' < 0 \text{ and } \phi' \geq 0 \\ (-A', \phi' + \pi) & \text{if } A' < 0 \text{ and } \phi' < 0 \end{cases} \tag{5.65}$$

Finally, we have assumed that $t_1 = 0$. Correspondingly, that means that t_2 can be expressed as $t_2 = N_2\Delta_t$ where N_2 is the (integer) number of time steps between the samples f_1 and f_2. Thus the argument of the trig functions above can be written as

$$\omega t_2 = 2\pi S_c \frac{N_2}{N_\lambda} \tag{5.66}$$

where N_λ is the number of points per wavelength of the excitation (and frequency of interest).

5.7 Conductivity

When a material is lossless, the phase constant β for a harmonic plane wave is given by $\omega\sqrt{\mu\epsilon}$ and the spatial dependence is given by $\exp(\pm j\beta x)$. When the material has a non-zero electrical conductivity ($\sigma \neq 0$), the material is lossy and the wave experiences exponential decay as it propagates. The spatial dependence is given by $\exp(\pm\gamma x)$ where

$$\gamma = j\omega\sqrt{\mu\epsilon\left(1 - j\frac{\sigma}{\omega\epsilon}\right)} = \alpha + j\beta \tag{5.67}$$

where α (the real part of γ) is the attenuation constant and β (the imaginary part of γ) is the phase constant. The attenuation and phase constants can be expressed directly in terms of the material parameters and the frequency:

$$\alpha = \frac{\omega\sqrt{\mu\epsilon}}{\sqrt{2}}\left(\left[1+\left(\frac{\sigma}{\omega\epsilon}\right)^2\right]^{1/2}-1\right)^{1/2}, \tag{5.68}$$

$$\beta = \frac{\omega\sqrt{\mu\epsilon}}{\sqrt{2}}\left(\left[1+\left(\frac{\sigma}{\omega\epsilon}\right)^2\right]^{1/2}+1\right)^{1/2}. \tag{5.69}$$

When the conductivity is zero, the attenuation constant is zero and the phase constant reduces to that of the lossless case, i.e., $\gamma = j\beta = j\omega\sqrt{\mu\epsilon}$.

Assume a wave is propagating in the positive x direction in a material with non-zero electrical conductivity. The wave amplitude will decay as $\exp(-\alpha x)$. The skin depth δ_{skin} is the distance over which the wave decays an amount $1/e$. Starting with a reference point of $x = 0$, the fields would have decayed an amount $1/e$ when x is $1/\alpha$ (so that the exponent is simply -1). Thus, δ_{skin} is given by

$$\delta_{\text{skin}} = \frac{1}{\alpha}. \tag{5.70}$$

Since the skin depth is merely a distance, it can be expressed in terms of the spatial step, i.e.,

$$\delta_{\text{skin}} = \frac{1}{\alpha} = N_L\Delta_x \tag{5.71}$$

where N_L is the number of spatial steps in the skin depth (think of the subscript L as standing for loss). N_L does not need to be an integer.

It is possible to use (5.68) to solve for the conductivity in terms of the attenuation constant. The resulting expression is

$$\sigma = \omega\epsilon\left(\left[1+\frac{2\alpha^2}{\omega^2\mu\epsilon}\right]^2-1\right)^{1/2}. \tag{5.72}$$

As shown in Sec. 3.12, when the electrical conductivity is non-zero the electric-field update equation contains the term $\sigma\Delta_t/2\epsilon$. Multiplying both side of (5.72) by $\Delta_t/2\epsilon$ yields

$$\frac{\sigma\Delta_t}{2\epsilon} = \frac{\omega\Delta_t}{2}\left(\left[1+\frac{2\alpha^2}{\omega^2\mu\epsilon}\right]^2-1\right)^{1/2}. \tag{5.73}$$

Assume that one wants to obtain a certain skin depth (or decay rate) at a particular frequency which is discretized with N_λ points per wavelength, i.e., $\omega = 2\pi f = 2\pi c/N_\lambda\Delta_x$. Thus the term $\omega\Delta_t/2$ can be rewritten

$$\frac{\omega\Delta_t}{2} = \frac{\pi}{N_\lambda}\frac{c\Delta_t}{\Delta_x} = \frac{\pi}{N_\lambda}S_c. \tag{5.74}$$

Similarly, using the same expression for ω and using $\alpha = 1/N_L\Delta_x$, one can write

$$\frac{2\alpha^2}{\omega^2\mu\epsilon} = \frac{2\left(\frac{1}{N_L\Delta_x}\right)^2}{\left(\frac{2\pi c}{N_\lambda\Delta_x}\right)^2\mu_0\mu_r\epsilon_0\epsilon_r} = \frac{N_\lambda^2}{2\pi^2N_L^2\epsilon_r\mu_r}. \tag{5.75}$$

Using (5.74) and (5.75) in (5.73) yields

$$\frac{\sigma\Delta_t}{2\epsilon} = \frac{\pi}{N_\lambda} S_c \left(\left[1 + \frac{N_\lambda^2}{2\pi^2 N_L^2 \epsilon_r \mu_r} \right]^2 - 1 \right)^{1/2}. \tag{5.76}$$

Note that neither the temporal nor the spatial steps appear in the right-hand side.

As an example how (5.76) can be used, assume that one wants a skin depth of $20\Delta_x$ for a wavelength of $40\Delta_x$. Thus $N_L = 20$ and $N_\lambda = 40$ and the skin depth is one half of the free-space wavelength. Further assume the Courant number S_c is unity, $\epsilon_r = 4$, and $\mu_r = 1$. Plugging these values into (5.76) yields $\sigma\Delta_t/2\epsilon = 0.0253146$.

Let us write a program where a TFSF boundary introduces a sine wave with a frequency that is discretized at 40 points per wavelength. We will only implement electrical loss (the magnetic conductivity is zero). Snapshots will be taken every time step after the temporal index is within 40 steps from the final time step. The lossy layer starts at node 100. To implement this program, we can re-use nearly all the code that was described in Sec. 4.9. To implement this, we merely have to change the `gridInit3()` function and the functions associated with the source function. The new `gridInit3()` function is shown in Program 5.1. The harmonic source function is given by the code presented in Program 5.2.

Program 5.1 `gridinitlossy.c` A `Grid` initialization function for modeling a lossy half space. Here the conductivity results in a skin depth of 20 cells for an excitation that is discretized using 40 cells per wavelength.

```
1  #include "fdtd3.h"
2
3  #define LOSS 0.0253146
4  #define LOSS_LAYER 100
5  #define EPSR 4.0
6
7  void gridInit3(Grid *g) {
8    double imp0 = 377.0;
9    int mm;
10
11   SizeX = 200;   // size of domain
12   MaxTime = 450; // duration of simulation
13   Cdtds = 1.0;   // Courant number
14
15   /* Allocate memory for arrays. */
16   ALLOC_1D(g->ez,   SizeX, double);
17   ALLOC_1D(g->ceze, SizeX, double);
18   ALLOC_1D(g->cezh, SizeX, double);
19   ALLOC_1D(g->hy,   SizeX - 1, double);
20   ALLOC_1D(g->chyh, SizeX - 1, double);
21   ALLOC_1D(g->chye, SizeX - 1, double);
22
```

```
23    /* set electric-field update coefficients */
24    for (mm=0; mm < SizeX; mm++)
25      if (mm < 100) {
26        Ceze(mm) = 1.0;
27        Cezh(mm) = imp0;
28      } else {
29        Ceze(mm) = (1.0 - LOSS) / (1.0 + LOSS);
30        Cezh(mm) = imp0 / EPSR / (1.0 + LOSS);
31      }
32
33    /* set magnetic-field update coefficients */
34    for (mm=0; mm < SizeX - 1; mm++) {
35      Chyh(mm) = 1.0;
36      Chye(mm) = 1.0 / imp0;
37    }
38
39    return;
40  }
```

Program 5.2 `ezincharm.c` Functions to implement a harmonic source. When initialized, the user is prompted to enter the number of points per wavelength (in the results to follow it is assumed the user enters 40).

```
1   #include "ezinc3.h"
2
3   /* global variables -- but private to this file */
4   static double ppw = 0, cdtds;
5
6   /* prompt user for source-function points per wavelength */
7   void ezIncInit(Grid *g){
8
9     cdtds = Cdtds;
10    printf("Enter points per wavelength: ");
11    scanf(" %lf", &ppw);
12
13    return;
14  }
15
16  /* calculate source function at given time and location */
17  double ezInc(double time, double location) {
18    if (ppw <= 0) {
19      fprintf(stderr,
20         "ezInc: must call ezIncInit before ezInc.\n"
21         "       Points per wavelength must be positive.\n");
```

```
22      exit(-1);
23    }
24
25    return sin(2.0 * M_PI / ppw * (cdtds * time - location));
26  }
```

Assuming the user specified that the TFSF boundary should be at node 50 and there should be 40 points per wavelength for the harmonic source, Fig. 5.2(a) shows the resulting maximum of the magnitude of the electric field as a function of position. For each position, all the snapshots were inspected and the maximum recorded. Figure 5.2(b) shows a superposition of 41 snapshots taken one time-step apart. One can see the exponential decay starting at node 100. Between node 50 and node 100 there is a standing-wave pattern caused by the interference of the incident and reflected waves. From the start of the grid to node 50 the magnitude is flat. This is caused by the fact that there is only scattered field here—there is nothing to interfere with the reflected wave and we see the constant amplitude associated with a pure traveling wave. The ratio of the amplitude at nodes 120 and 100 was found to be 0.3644 whereas the ideal value of $1/e$ is 0.3679 (thus there is approximately a one percent error in this simulation).

If one were interested in non-zero magnetic conductivity σ_m, the loss term which appears in the magnetic-field update equations is $\sigma_m \Delta_t / 2\mu$. This term can be handled in exactly the same way as the term resulting from electric conductivity.

5.8 Example: Obtaining the Transmission Coefficient for a Planar Interface

In this last section, we demonstrate how the transmission coefficient for a planar dielectric boundary can be obtained from the FDTD method. This serves to highlight many of the points that were considered in the previous section. We will compare the results to the exact solution. The disparity between the two provides motivation to determine the dispersion relation in the FDTD (which is covered in Chap. 7).

The majority of instructional material concerning electromagnetics is expressed in terms of harmonic, or frequency-domain, signals. A temporal dependence of $\exp(j\omega t)$ is understood and therefore one only has to consider the spatial variation. In the frequency domain, the fields and quantities such as the propagation constant and the characteristic impedance are represented by complex numbers. These complex numbers give the magnitude and phase of the value and will be functions of frequency. In the following discussion a caret (hat) will be used to indicate a complex quantity and one should keep in mind that complex numbers are inherently tied to the frequency domain. Given the frequency-domain representation of the field at a point, the temporal signal is recovered by multiplying by $\exp(j\omega t)$ and taking the real part. Thus a 1D harmonic field propagating in the $+x$ direction could be written in any of these equivalent forms

$$E_z(x,t) = \Re\left[\hat{E}_z^+(x,t)\right] = \Re\left[\hat{E}_z^+(x)e^{j\omega t}\right] = \Re\left[\hat{E}_0^+ e^{-\hat{\gamma}x} e^{j\omega t}\right] = \Re\left[\hat{E}_0^+ e^{-(\alpha+j\beta)x} e^{j\omega t}\right], \quad (5.77)$$

where $\Re[]$ indicates the real part. $\hat{E}_z^+(x)$ is the frequency-domain representation of the field (i.e., a phasor that is a function of position), $\hat{\gamma}$ is the propagation constant which has a real part α and

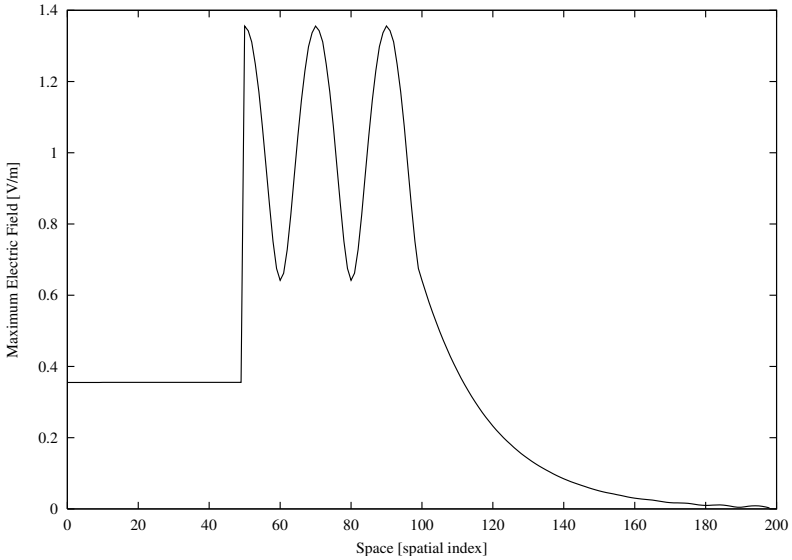

(a)

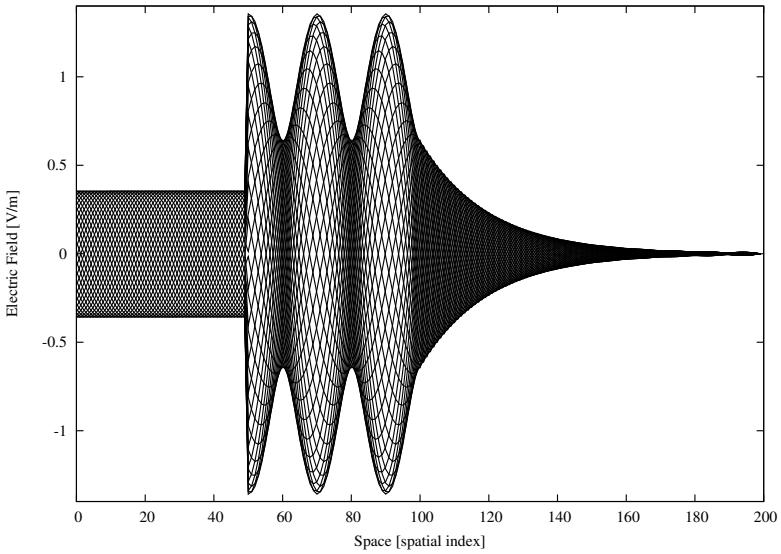

(b)

Figure 5.2: (a) Maximum electric field magnitude that exists at each point (obtained by obtaining the maximum value in all the snapshots). The flat line over the first 50 nodes corresponds to the scattered-field region. The reflected field travels without decay and hence produces the flat line. The total-field region between nodes 50 and 100 contains a standing-wave pattern caused by the interference of the incident and scattered fields. There is exponential decay of the fields beyond node 100 which is where the lossy layer starts. (b) Superposition of 41 individual snapshots of the field which illustrates the envelope of the field.

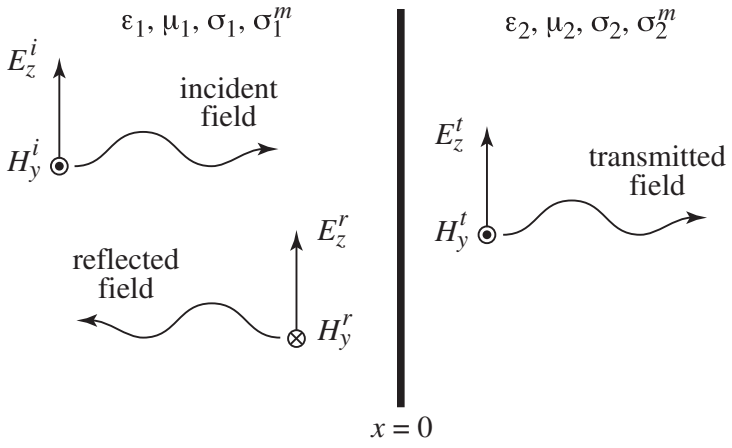

Figure 5.3: Planar interface between two media. The interface is at $x = 0$ and a wave is incident on the interface from the left. When the impedances of the two media are not matched, a reflected wave must exist in order to satisfy the boundary conditions.

an imaginary part β, and $\hat{E}_0^+$ is a complex constant that gives the amplitude of the wave (it is independent of position; the superscript "+" is merely used to emphasize that we are discussing a wave propagating in the $+x$ direction). Note that if more than a single frequency is present, $\hat{E}_0^+$ does not need to be the same for each frequency.

More generally, $\hat{E}_0^+$ will be a function of frequency (we could write this expressly as $\hat{E}_0^+(\omega)$ but the caret implicitly indicates dependence on frequency). To construct a temporal that consists of a multiple frequencies, or even a continuous spectrum of frequencies, one must sum the contributions from each frequency such as is done with a Fourier integral.

In FDTD simulations the time-domain form of the signal is obtained directly. However, one often is interested in the behavior of the fields as a function of frequency. As has been discussed in Sec. 5.3, one merely has to take the Fourier transform of a signal to obtain its spectral content. This transform, by itself, is typically of little use. One has to normalize the signal in some way. Knowing what came out of a system is rather meaningless unless one knows what went into the system. Here we will work through a couple of simple examples to illustrate how a broad range of spectral information can be obtained from FDTD simulations.

5.8.1 Transmission through a Planar Interface (Continuous World)

Consider the planar interface at $x = 0$ between two media as depicted in Fig. 5.3. We restrict consideration to electric polarization in the z direction and assume the incident field originates in the first medium. In the frequency domain, the incident, reflected, and transmitted fields are given by

$$\hat{E}_z^i(x) = \hat{E}_{a1}^+ e^{-\hat{\gamma}_1 x} \quad \text{incident,} \tag{5.78}$$

$$\hat{E}_z^r(x) = \hat{E}_{a1}^- e^{+\hat{\gamma}_1 x} = \hat{\Gamma}\hat{E}_{a1}^+ e^{+\hat{\gamma}_1 x} \quad \text{reflected,} \tag{5.79}$$

$$\hat{E}_z^t(x) = \hat{E}_{a2}^+ e^{-\hat{\gamma}_2 x} = \hat{T}\hat{E}_{a1}^+ e^{-\hat{\gamma}_2 x} \quad \text{transmitted,} \tag{5.80}$$

where $\hat{\Gamma}$ is the reflection coefficient, $\hat{T}$ is the transmission coefficient, and $\hat{\gamma}_n$ is the propagation constant given by $j\omega\sqrt{\mu_n(1-j\sigma_n^m/\omega\mu_n)\epsilon_n(1-j\sigma_n/\omega\epsilon_n)}$ where the n indicates the medium and σ^m is the magnetic conductivity. The amplitude of the incident field $\hat{E}_{a1}^+$ is, in general, complex and a function of frequency. By definition $\hat{\Gamma}$ and $\hat{T}$ are

$$\hat{\Gamma} = \left.\frac{\hat{E}_z^r(x)}{\hat{E}_z^i(x)}\right|_{x=0} = \frac{\hat{E}_{a1}^-}{\hat{E}_{a1}^+}, \tag{5.81}$$

$$\hat{T} = \left.\frac{\hat{E}_z^t(x)}{\hat{E}_z^i(x)}\right|_{x=0} = \frac{\hat{E}_{a2}^+}{\hat{E}_{a1}^+}. \tag{5.82}$$

The fact that these are defined at $x = 0$ is important.

The magnetic field is related to the electric field by

$$\hat{H}_y^i(x) = -\frac{1}{\hat{\eta}_1}\hat{E}_z^i(x), \tag{5.83}$$

$$\hat{H}_y^r(x) = \frac{1}{\hat{\eta}_1}\hat{E}_z^r(x), \tag{5.84}$$

$$\hat{H}_y^t(x) = -\frac{1}{\hat{\eta}_2}\hat{E}_z^t(x), \tag{5.85}$$

where the characteristic impedance $\hat{\eta}_n$ is given by $\sqrt{\mu_n(1-j\sigma_n^m/\omega\mu_n)/\epsilon_n(1-j\sigma_n/\omega\epsilon_n)}$. Since the magnetic and electric fields are purely tangential to the planar interface, the sum of the incident and reflected field at $x = 0$ must equal the transmitted field at the same point. Matching the boundary condition on the electric field yields

$$1 + \hat{\Gamma} = \hat{T}, \tag{5.86}$$

while matching the boundary conditions on the magnetic field produces

$$\frac{1}{\hat{\eta}_1}(1 - \hat{\Gamma}) = \frac{1}{\hat{\eta}_2}\hat{T}. \tag{5.87}$$

Solving these for $\hat{T}$ yields

$$\hat{T} = \frac{2\hat{\eta}_2}{\hat{\eta}_1 + \hat{\eta}_2}. \tag{5.88}$$

Using this in (5.86) the reflection coefficient is found to be

$$\hat{\Gamma} = \frac{\hat{\eta}_2 - \hat{\eta}_1}{\hat{\eta}_2 + \hat{\eta}_1}. \tag{5.89}$$

5.8.2 Measuring the Transmission Coefficient Using FDTD

Now consider two FDTD simulations. The first simulation will be used to record the incident field. In this simulation the computational domain is homogeneous and the material properties correspond to that of the first medium. The field is recorded at some observation point x_1. Since nothing is present to interfere with the incident field, the recorded field will be simply the incident

field at this location, i.e, $E_z^i(x_1,t)$. In the second simulation, the second medium is present. We record the fields at the same observation point but we ensure the point was chosen such that it is located in the second medium (i.e., the interface is to the left of the observation point). Performing an FDTD simulation in this case yields the transmitted field $E_z^t(x_1,t)$. The goal now is to obtain the transmission coefficient using the temporal recordings of the field obtained from these two simulations.

Note that in this section we will not distinguish between the way in which field propagate in the continuous world and the way in which they propagate in the FDTD grid. In Chap. 7 we will discuss in some detail how these differ.

One cannot use $E_z^t(x_1,t)/E_z^i(x_1,t)$ to obtain the transmission coefficient. The transmission coefficient is inherently a frequency-domain concept and currently we have time-domain signals. The division of these temporal signals is essentially meaningless (e.g., the result is undefined when the incident signal is zero).

The incident and transmitted fields must be converted to the frequency domain using a Fourier transform. Thus one obtains

$$\hat{E}_z^i(x_1) = \mathcal{F}\left(E_z^i(x_1,t)\right), \tag{5.90}$$

$$\hat{E}_z^t(x_1) = \mathcal{F}\left(E_z^t(x_1,t)\right), \tag{5.91}$$

where $\mathcal{F}$ indicates the Fourier transform. The division of these two functions *is* meaningful—at least at all frequencies where $\hat{E}_z^i(x_1)$ is non-zero. (At frequencies where $\hat{E}_z^i(x_1)$ is zero, there is no incident spectral energy and hence one cannot obtain the transmitted field at those particular frequencies. In practice it is relatively easy to introduce energy into an FDTD grid that spans a broad range of frequencies.)

Since the observation point was not specified to be on the boundary, the ratio of these field fields is

$$\frac{\hat{E}_z^t(x_1)}{\hat{E}_z^i(x_1)} = \frac{\hat{E}_{a2}^+ e^{-\hat{\gamma}_2 x_1}}{\hat{E}_{a1}^+ e^{-\hat{\gamma}_1 x_1}} = \frac{\hat{E}_{a2}^+}{\hat{E}_{a1}^+} e^{(\hat{\gamma}_1-\hat{\gamma}_2)x_1} = \hat{T} e^{(\hat{\gamma}_1-\hat{\gamma}_2)x_1}. \tag{5.92}$$

Solving this for $\hat{T}$ yields

$$\hat{T}(\omega) = e^{(\hat{\gamma}_2-\hat{\gamma}_1)x_1} \frac{\hat{E}_z^t(x_1)}{\hat{E}_z^i(x_1)}. \tag{5.93}$$

To demonstrate how the transmission coefficient can be reconstructed from FDTD simulations, let us consider an example where the first medium is free space and the second one has a relative permittivity ϵ_r of 9. In this case $\hat{\gamma}_1 = j\omega\sqrt{\mu_0\epsilon_0} = j\beta_0$ and $\hat{\gamma}_2 = j\omega\sqrt{\mu_0 9\epsilon_0} = j3\beta_0$. Therefore (5.93) becomes

$$\hat{T}(\omega) = e^{j(3\beta_0-\beta_0)x_1} \frac{\hat{E}_z^t(x_1)}{\hat{E}_z^i(x_1)} = e^{j2\beta_0 x_1} \frac{\hat{E}_z^t(x_1)}{\hat{E}_z^i(x_1)}. \tag{5.94}$$

The terms in the exponent can be written

$$2\beta_0 x_1 = 2\frac{2\pi}{\lambda}x_1 = \frac{4\pi}{N_\lambda \Delta_x} N_1 \Delta_x = \frac{4\pi}{N_\lambda} N_1 \tag{5.95}$$

where N_1 is the number of spatial steps between the interface and the observation point at x_1 and, as was discussed in Chap. 5, N_λ is the number of spatial steps per a free-space wavelength of λ.

The continuous-world transmission coefficient can be calculated quite easily from (5.88) and this provides a reference solution. Ideally the FDTD simulation would yield this same value for all frequencies. For this particular example the characteristic impedance of the first medium is $\hat{\eta}_1 = \eta_0$ while for the second medium it is $\hat{\eta}_2 = \eta_0/3$. Thus the transmission coefficient is

$$\hat{T}_{\text{exact}} = \frac{2\eta_0/3}{\eta_0 + \eta_0/3} = 1/2. \tag{5.96}$$

Note that this is a real number and independent of frequency (so the tilde on T is somewhat misleading).

For the FDTD simulations, let us record the field 80 spatial steps away from the interface, i.e., $N_1 = 80$, and run the simulation for 8192 time steps, i.e., $N_T = 8192$. The simulation is run at the Courant limit $S_c = 1$. The source is a Ricker wavelet discretized so that the peak spectral content exists at 50 points per wavelength ($N_P = 50$). From Sec. 5.3, recall the relationship between the points per wavelength N_λ and frequency index N_{freq} which is repeated below:

$$N_{\text{freq}} = \frac{N_T}{N_\lambda} S_c. \tag{5.97}$$

With a Courant number of unity and 8192 time steps, the points per wavelength for any given frequency (or spectral index) is given by

$$N_\lambda = \frac{8192}{N_{\text{freq}}}. \tag{5.98}$$

Combining this with (5.93) and (5.95) yields

$$\hat{T}_{\text{FDTD}} = e^{j\left(\frac{4\pi N_1 N_{\text{freq}}}{8192}\right)} \frac{\hat{E}_z^t(x_1)}{\hat{E}_z^i(x_1)}. \tag{5.99}$$

Ideally (5.96) and (5.99) will agree at all frequencies. To see if that is the case, Fig. 5.4 shows three plots related to the incident and transmitted fields. Figure 5.4(a) shows the first 500 time steps of the temporal signals recorded at the observation point both with and without the interface present (i.e., the transmitted and incident fields, respectively). Figure 5.4(b) shows the magnitude of the Fourier transforms of the incident and transmitted fields for the first 500 frequencies. Since a Ricker wavelet was used, the spectra are essentially in accordance with the discussion of Sec. 5.2.3. There is no spectral energy at dc and the spectral content exponentially approaches zero at high frequencies.

Figure 5.4(c) plots the magnitude of the ratio of the transmitted and incident field as a function of frequency. Ideally this would be $1/2$ for all frequencies. Note the rather small vertical scale of the plot. Near dc the normalized transmitted field differs rather significantly from the ideal value, but this is in a region where the results should not be trusted because there is not enough incident energy at these frequencies. At the higher frequencies some oscillations are present. The normalized field generally remains within two percent of the ideal value over this range of frequencies.

Figure 5.5(a) provides the same information as Fig. 5.4(c) except now the result is plotted versus the discretization N_λ. In this figure dc is off the scale to the right (since in theory dc has an infinite number of points per wavelength). As the frequency goes up, the wavelength gets shorter

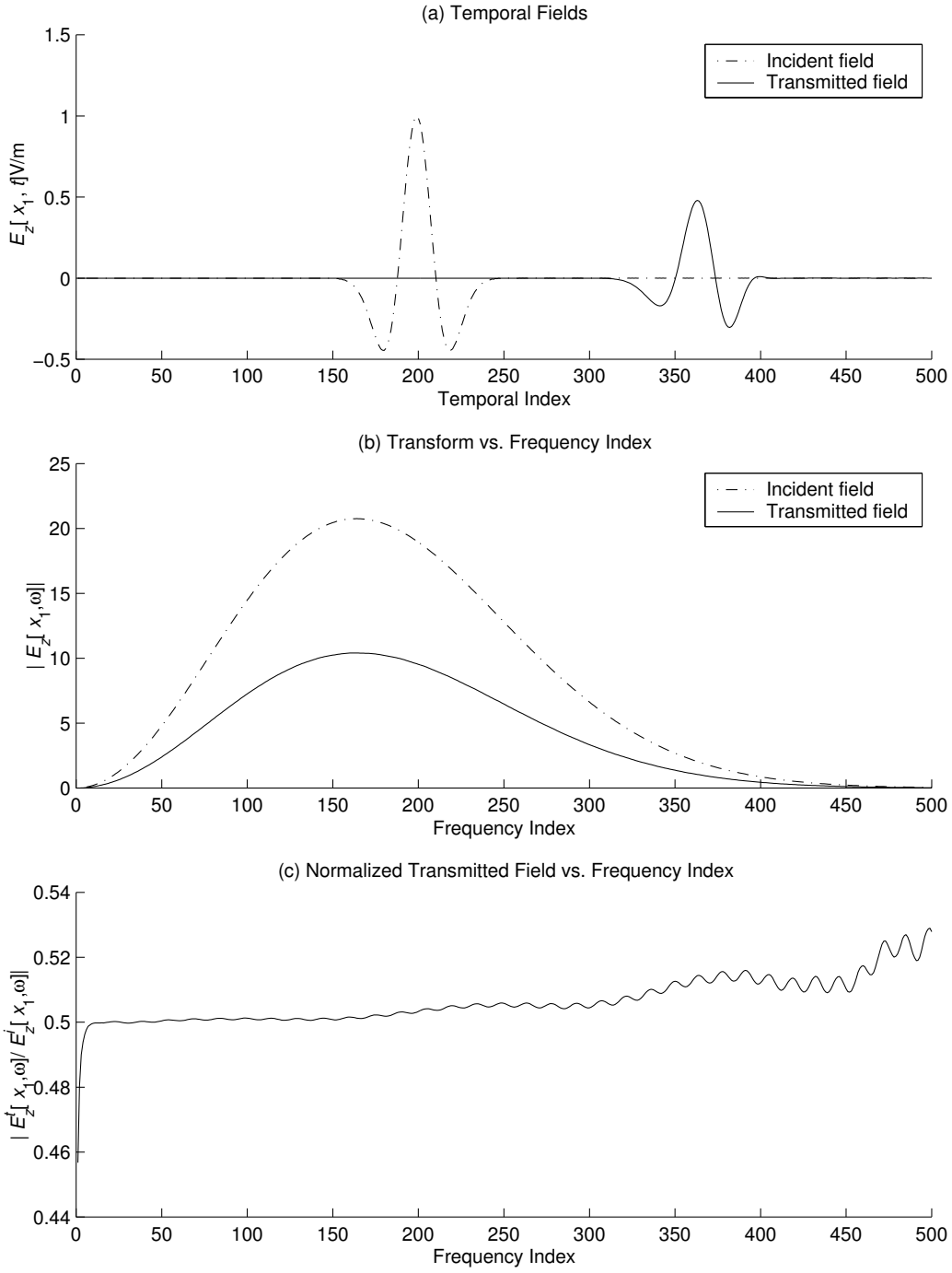

Figure 5.4: (a) Time-domain fields at the observation point both with and the without the interface present. The field without the interface is the incident field and the one with the interface is the transmitted field. (b) Magnitude of the Fourier transforms of the incident and transmitted fields. The transforms are plotted versus the frequency index N_{freq}. It can be seen that the fields do not have much spectral content near dc nor at high frequencies. (c) Magnitude of the transmitted field normalized by the incident field versus the frequency index. Ideally this would be $1/2$ for all frequencies. Errors are clearly evident when the spectral content of the incident field is small.

and hence the number of points per wavelength decreases. Thus high frequencies are to the left and low frequencies are to the right. The highest frequency in this plot corresponds to an N_{freq} of 500. In terms of the discretization, this is $N_\lambda = N_T/N_{\text{freq}} = 16.384$. This may not seem like a particularly coarse discretization, but one needs to keep in mind that this is the discretization in frees pace. Within the dielectric, which here has $\epsilon_r = 9$, the wavelength is three times smaller and hence within the dielectric the fields are only discretized at approximately five points per wavelength (which is considered a very coarse discretization). From this figure it is clear that the FDTD simulations provide results which are close to the ideal over a fairly broad range of frequencies.

Figure 5.5(b) shows the real and imaginary part of the reflection coefficient, i.e., $\hat{T}_{\text{FDTD}}$ defined in (5.99), as a function of the discretization. Ideally the imaginary part would be zero and the real part would be $1/2$. As can be seen, although the magnitude of the transmission coefficient is nearly $1/2$ over the entire spectrum, the phase differs rather significantly as the discretization decreases (i.e., the frequency increases).

The Matlab code used to generate Fig. 5.4 is shown in Program 5.3 while the code which generated Fig. 5.5 is given in Program 5.4. It is assumed the incident field from the FDTD simulation is recorded to a file named `inc-8192` while the transmitted field, i.e., the field when the dielectric is present, is recorded in `die-8192`. The code in Program 5.3 has to be run prior to that of 5.4 in order to load and initialize the data.

Let us now consider the same scenario but let the observation point be four steps away from the boundary instead of 80, i.e., $N_1 = 4$. Following the previous steps, the incident and transmitted fields are recorded, their transforms are taken, then divided, and finally the phase is adjusted to obtain the transmission coefficient. The result for this observation point is shown in Fig. 5.6. The real and imaginary parts stay closer to the ideal values over a larger range of frequencies than when the observation point was 80 cells from the boundary. The fact that the quality of the results are frequency sensitive as well as sensitive to the observation point is a consequence of numeric dispersion in the FDTD grid, i.e., different frequencies propagate at different speeds. (This is the subject of Chap. 7.)

Program 5.3 Matlab session used to generate Fig. 5.4.

```
incTime = dlmread('inc-8192'); % incident field file
dieTime = dlmread('die-8192'); % transmitted field file

inc = fft(incTime);  % take Fourier transforms
die = fft(dieTime);

nSteps = length(incTime);  % number of time steps
freqMin = 1;    % minimun frequency index of interest
freqMax = 500;  % maximum frequency of interest
freqIndex = freqMin:freqMax; % range of frequencies of interest
% correct for offset of 1 in matlab's indexing
freqSlice = freqIndex + 1;
courantNumber = 1;
% points per wavelength for freqencies of interest
```

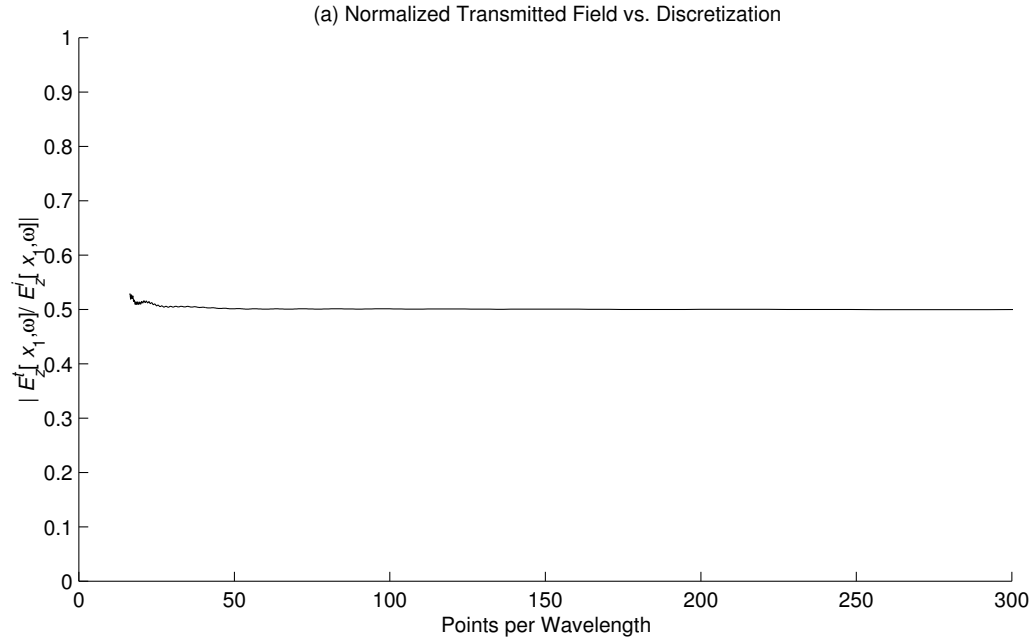

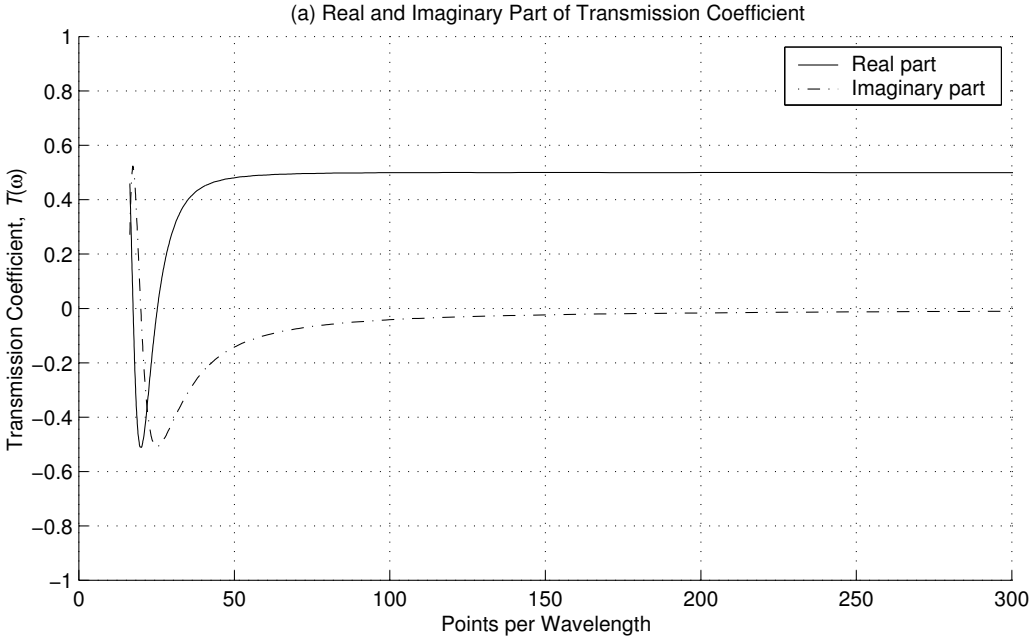

Figure 5.5: (a) The magnitude of the normalized transmitted field as a function of the (free space) discretization N_λ. Ideally this would be $1/2$ for all discretizations. (b) Real and imaginary part of the transmission coefficient transformed back to the interface $x = 0$ versus discretization. Ideally the real part would be $1/2$ and the imaginary part would be zero for all discretization. For these plots the observation point was 80 cells from the interface ($N_1 = 80$).

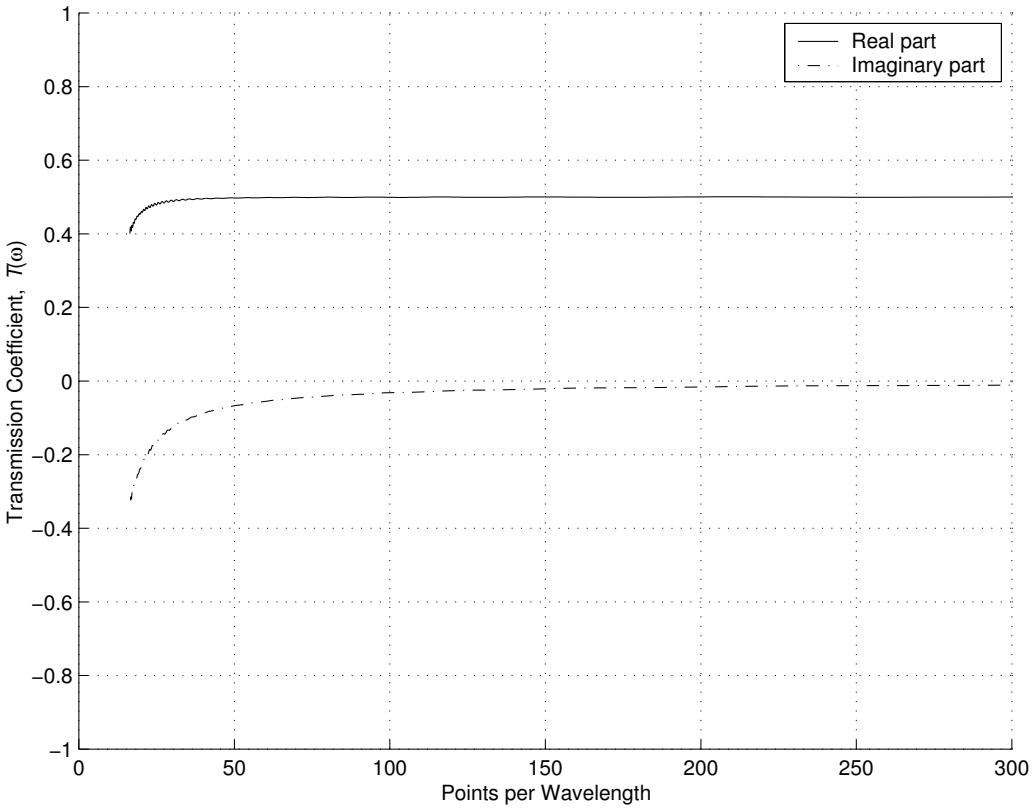

Figure 5.6: Real and imaginary part of the transmission coefficient transformed back to the interface $x = 0$ versus discretization. Ideally the real part would be $1/2$ and the imaginary part would be zero for all discretization. The observation point was four cells from the interface ($N_1 = 4$).

```
nLambda = nSteps ./ freqIndex * courantNumber;
clf
subplot(3, 1, 1)
hold on
plot(incTime(freqSlice), '-.');
plot(dieTime(freqSlice));
legend('Incident field', 'Transmitted field');
xlabel('Temporal Index');
ylabel('{\it E_z}[{\it x}_1,{\it t}] V/m');
title('(a) Temporal Fields');

subplot(3,1,2)
hold on
plot(freqIndex, abs(inc(freqSlice)), '-.');
plot(freqIndex, abs(die(freqSlice)));
legend('Incident field', 'Transmitted field');
xlabel('Frequency Index');
ylabel('|{\it E_z}[{\it x}_1,\omega]|');
title('(b) Transform vs. Frequency Index');
hold off

subplot(3, 1, 3)
hold on
plot(freqIndex, abs(die(freqSlice) ./ inc(freqSlice)));
xlabel('Frequency Index');
ylabel('|{\it E^t_z}[{\it x}_1,\omega]/...
                          {\it E^i_z}[{\it x}_1,\omega]|');
title('(c) Normalized Transmitted Field vs. Frequency Index');
hold off
```

Program 5.4 Matlab session used to generate Fig. 5.5. The commands shown in Program 5.3 would have to be run prior to these commands in order to read the data, generate the Fourier transforms, etc.

```
clf

subplot(2, 1, 1)
hold on
plot(nLambda, abs(die(freqSlice) ./ inc(freqSlice)));
xlabel('Points per Wavelength');
ylabel('|{\it E^t_z}[{\it x}_1,\omega]/...
                          {\it E^i_z}[{\it x}_1,\omega]|');
title('(a) Normalized Transmitted Field vs. Discretization');
axis([0 300 0 1])
```

```
hold off

% Array obtained from exp() must be transposed to make arrays
% conformal.  Simply using ' (a prime) for trasposition will yield
% the conjugate transpose.  Instead, use .' (dot-prime) to get
% transposition without conjugation.
subplot(2, 1, 2)
hold on
plot(nLambda, real(exp(j*pi*freqIndex/25.6).' .* ...
                   die(freqSlice) ./ inc(freqSlice)));
plot(nLambda, imag(exp(j*pi*freqIndex/25.6).' .* ...
                   die(freqSlice) ./ inc(freqSlice)), '-.');
xlabel('Points per Wavelength');
ylabel('Transmission Coefficient, {\it T}(\omega)');
title('(b) Real and Imaginary Part of Transmission Coefficient');
legend('Real part', 'Imaginary part');
axis([0 300 -1 1])
grid on
hold off
```

Although we have only considered the transmission coefficient in this example, the reflection coefficient could be obtained in a similar fashion. We have intentionally considered a very simple problem in order to be able to compare easily the FDTD solution to the exact solution. However one should keep in mind that the FDTD method could be used to analyze the reflection or transmission coefficient for a much more complicated scenario, e.g., one in which the material properties varied continuously, and perhaps quite erratically (with some discontinuities present), over the transition from one half-space to the next. Provided a sufficiently small spatial step-size was used, the FDTD method can solve this problem with essentially no more effort than was used to model the abrupt interface. However, to obtain the exact solution, one may have to work much harder.